D19

19

APPLICATION OF NUMERICAL OPTIMIZATION TO THE DESIGN OF ADVANCED SUPERCRITICAL AIRFOILS

Raymond R. Johnson
Vought Corporation

Raymond M. Hicks
NASA Ames Research Center

SUMMARY

A recent application of numerical optimization to the design of advanced airfoils for transonic aircraft has shown that low-drag sections can be developed for a given design Mach number without an accompanying drag increase at lower Mach numbers. This is achieved by imposing a constraint on the drag coefficient at an off-design Mach number while minimizing the drag coefficient at the design Mach number. This multiple design-point numerical optimization has been implemented with the use of airfoil shape functions which permit a wide range of attainable profiles during the optimization process. Analytical data for the starting airfoil shape, a single design-point optimized shape, and a double design-point optimized shape are presented. Experimental data obtained in the NASA Ames Two-by Two-Foot Wind Tunnel are also presented and discussed.

INTRODUCTION

The design of supercritical airfoils for advanced high speed aircraft has been facilitated by the computerized analytical methods which have been developed in recent years. Although these methods provide good performance predictions for each individual design point which is considered, they do not allow the designer to automatically consider off-design characteristics during the design process. A method which does provide multiple design-point capability is described in reference 1. It is based on design by numerical optimization. An application of that method to a single design-point and a double design-point airfoil optimization is addressed in the present study. The double design-point optimization produced a low drag supercritical airfoil for a given Mach number subject to a drag constraint at a lower Mach number.

The treatment of the supercritical airfoil design problem by this method has been facilitated by the development of a set of airfoil shape functions (reference 1) which provide a wide range of attainable profiles during the design process. The coefficients of these shape functions are used as design variables in the numerical optimization technique which consists of two existing computer codes: (a) an optimization program based on the method of

feasible directions (reference 2) and (b) an aerodynamic analysis program based on an iterative solution of the full potential equation for transonic flow (reference 3).

SYMBOLS

a_i	shape function coefficients
c	chord
C_D	section drag coefficient
C_l	section lift coefficient
C_m	section pitching moment coefficient
C_p	pressure coefficient
f_i	airfoil shape functions
M	Mach number
X	airfoil abscissa
Y	airfoil ordinate

DESIGN METHOD

Only a brief description of numerical optimization will be given here. A complete discussion of the technique can be found in reference 4.

A schematic flow chart of the numerical optimization design program used during this study is shown in figure 1. A baseline airfoil is required to start each design problem. The airfoil shape is represented in the program by the following equation:

$$Y = Y_{basic} + \sum_i a_i f_i$$

where Y_{basic} is the set of ordinates of the baseline airfoil and f_i are the shape functions. The shape functions are added linearly to the baseline profile by the optimization program to achieve the desired design improvement. The contribution of each function is determined by the value of the coefficient, a_i, associated with that function. These a_i coefficients are therefore the design variables. Other inputs to the program include Mach number, angle of attack, and any constraints to be imposed on the design.

The hypothetical design problem represented by the flow chart is drag minimization at one Mach number, M_1, with drag constrained to some specified value at another Mach number, M_2. The optimization program begins by changing the design variables, one by one, from the initial value of zero to 0.001. It returns to the aerodynamics program for evaluation of the drag coefficient at both Mach numbers M_1 and M_2 after each change. The value of 0.001 is somewhat arbitrary but has been found to be an effective step change in the design variables to calculate the required partial derivatives. The partial derivatives of drag with respect to each design variable form the gradient of drag, ∇C_d. The direction in which the design variables are changed to reduce the drag coefficient at M_1 is $-\nabla C_d$ (the steepest descent direction) if the drag constraint at M_2 is not active. The optimization program then increments the design variables in this direction until the drag starts to increase because of nonlinearity in the design space or the drag constraint at Mach number M_2 is encountered. If either of these possibilities occurs, new gradients are calculated and a new direction is found that will decrease drag without violating the constraint. When a minimum value of drag for Mach number M_1 is attained with a satisfied drag constraint at M_2, the required optimized airfoil has been achieved.

AIRFOIL SHAPE FUNCTIONS

Supercritical airfoil design by numerical optimization is facilitated by using a set of geometric shape functions, each of which affects a different limited region of the profile. General classes of such functions which have been used successfully to optimize supercritical airfoils are described in reference 1. The shape functions that were used in the present study were selected from those general functions and were applied to the airfoil upper surface only. The exponential decay function and the sine functions are presented in figure 2. The exponential decay function, f_1, provided variations in curvature near the airfoil leading edge. In the sine functions, the exponents on the chordwise coordinate, x, were assigned so that the maximum perturbations of f_2, f_3, f_4 and f_5 were at 20, 40, 60, and 80 percent of the chord respectively. The width of the region affected by each sine function was controlled by the localization power, 3. Previous studies (reference 1) have found that these shape functions provide a broad range of smooth airfoil contour modifications during the optimization process.

ANALYTICAL DESIGN RESULTS AND DISCUSSION

The importance of considering off-design performance of an airfoil during the design process will be illustrated by comparing the results of a single design-point optimization with a double design-point optimization. The first involves recontouring the upper surface of an existing supercritical airfoil to reduce the wave drag at a single design Mach number. The second consists of recontouring the upper surface of the same airfoil to reduce the wave drag at the design Mach number subject to a drag constraint at a lower Mach number.

The calculated wave drag (reference 3) for Mach numbers near drag divergence for the starting airfoil and the two optimized airfoils are presented in figure 3. All these data are for 0.40 C_l, the design lift coefficient of the starting airfoil. Mach number 0.78 was arbitrarily selected as the primary design point, i.e., the Mach number at which the drag would be minimized. Results of the single design point optimization are indicated as 412M1. The drag at Mach number 0.78 is significantly less than that of the starting airfoil and as a result the drag rise occurs at a higher Mach number. However, the drag at lower Mach numbers, 0.76 and 0.77, is greater than that of the starting airfoil. This local region of drag-creep could limit the usefulness of the improved drag rise characteristics of the optimized airfoil.

In order to avoid the drag-creep problem, the airfoil was optimized a second time with an upper bound of .0005 imposed on the drag coefficient at Mach number 0.77. Results of this double design-point optimization are indicated in figure 3 as 412M2. The drag rise for this airfoil occurs at a slightly lower Mach number than it does for 412M1, but there is no drag-creep over the range of Mach numbers for which the airfoils were analyzed. Therefore, airfoil 412M2 is the more desirable design.

Chordwise pressure distributions for the starting airfoil and for airfoil 412M2 at Mach number 0.77 are presented in figure 4. The reason for the lower wave drag of the optimized airfoil is obvious. The starting airfoil has a well developed shock at approximately 40 percent of the chord, but airfoil 412M2 does not. Instead, it exhibits a gradual recompression from approximately 10 percent to 50 percent of the chord. The geometric modification which has produced the pressure distribution change is shown in figure 5. This modification is primarily a reduction in surface curvature from 5 percent to 40 percent of the chord.

The aerodynamics code that was used in the optimization program is an inviscid, potential flow analysis method. In order to account for first order viscous effects in the flow field solution, a boundary layer displacement thickness was added to the starting profile before the optimization process. The displacement thickness was calculated for the pressure distribution of the starting airfoil at a Mach number near its design condition, 0.78. It remained unchanged throughout the optimization process, and each of the optimized airfoils included this same passive displacement thickness. Therefore, the analytical characteristics of the airfoils did not reflect potential changes in boundary layer behavior due to changes in the chordwise pressure distributions.

Another aerodynamic analysis code (reference 5) was used to evaluate the active boundary layer characteristics of the starting airfoil and optimized airfoil 412M2. That computer program is also based on an iterative solution of the full potential equation for transonic flow, and it includes a momentum-integral calculation of the turbulent boundary layer parameters. During the solution, the airfoil geometry is regularly updated with the boundary layer displacement thickness. The results of the viscous analyses with that code for Mach numbers between 0.76 and 0.81 indicated that the differences in boundary layer characteristics would be small. The calculated

wave drag for the starting airfoil and airfoil 412M2 is presented in figure 6. The relative increase in the drag rise Mach number is in good agreement with the results of the inviscid code (figure 3).

EXPERIMENTAL RESULTS

Models of the starting airfoil and airfoil 412M2 were tested in the NASA Ames Two-by Two-Foot Wind Tunnel. Data were obtained at angles of attack from -4° to stall at Mach numbers from 0.20 to 0.81. The test Reynolds number varied with Mach number as presented in Table I. Preliminary data from the test are presented in figures 7 and 8. The incremental values of drag coefficient, C_D, have been referenced to the minimum drag measured for either of the airfoils at each lift coefficient. Thereby, extraneous components in the absolute drag level have been excluded from the comparison.

Drag characteristics for the starting airfoil and airfoil 412M2 at lift coefficient 0.40 (figure 7) indicate a difference in drag rise Mach number of 0.02 to 0.03. This improvement is greater than had been predicted by the analytical codes (figures 3 and 6). Drag characteristics for the two airfoils at lift coefficient 0.60 (figure 8) also indicate significantly less drag for the optimized airfoil 412M2 at all Mach numbers. Therefore the airfoil performance at this off-design condition has not been adversely affected by the design improvement at 0.40 lift coefficient.

The low speed drag-creep which occurs between Mach numbers 0.60 and 0.70 for both airfoils is caused by the initial development of supercritical velocities over the upper surface and the formation of a mild shock near the leading edge. Only Mach numbers greater than 0.76 were considered during the present analytical design study, but the numerical optimization technique could also be applied to the minimization of drag-creep at the lower speeds.

CONCLUDING REMARKS

A technique for designing low-drag supercritical airfoils has been demonstrated. The technique was used to modify the upper surface of an existing 12 percent thick supercritical section to achieve a substantial drag reduction at Mach number 0.78 without an accompanying drag increase at lower Mach numbers. The ability to treat this and other multiple design-point problems has been achieved by the use of a set of airfoil shape functions which provide the necessary flexibility in the profiles that are attainable by the numerical optimization design technique. Such capability is important because each design point might require the modification of a different region of the profile.

The two design-point problem considered in the present study illustrates the advantage of design by numerical optimization. Aerodynamic requirements at any number of off-design conditions are handled automatically without manual intervention by the designer. Therefore, it provides a powerful tool for the

design of airfoils to meet specified performance goals throughout a flight envelope.

REFERENCES

1. Hicks, R. M.; Vanderplaats, G. N.: Application of Numerical Optimization to the Design of Supercritical Airfoils without Drag-Creep. SAE Paper 770440, 1977.

2. Vanderplaats, G. N.: CONMIN-A Fortran Program for Constrained Function Minimization. NASA TM X-62,282, 1973.

3. Jameson, A.: Iterative Solution of Transonic Flows over Airfoils and Wings Including Flows at Mach 1. Comm. Pure Appl. Math., Vol. 27, pp 283-309, 1974.

4. Vanderplaats, G. N.; Hicks, R. M.; Murman, E. M.: Application of Numerical Optimization Techniques to Airfoil Design. NASA SP-347, Part II, 1975.

5. Bauer, F.; Garabedian, P.; Korn, D.; Jameson, A.: Supercritical Wing Sections II. Lecture Notes in Economics and Mathematical Systems, Vol. 108, Springer-Verlag, 1975.

TABLE I. - WIND TUNNEL TEST PARAMETERS

Mach Number	Angle of Attack Range	Reynolds Number
0.20	-4^{o} to stall	1.9×10^{6}
0.40	↓	3.0×10^{6}
0.60	↓	4.0×10^{6}
0.70	↓	↓
0.75	↓	↓
0.76	↓	↓
0.77	↓	↓
0.78	↓	↓
0.79	↓	↓
0.80	↓	↓
0.81	↓	↓

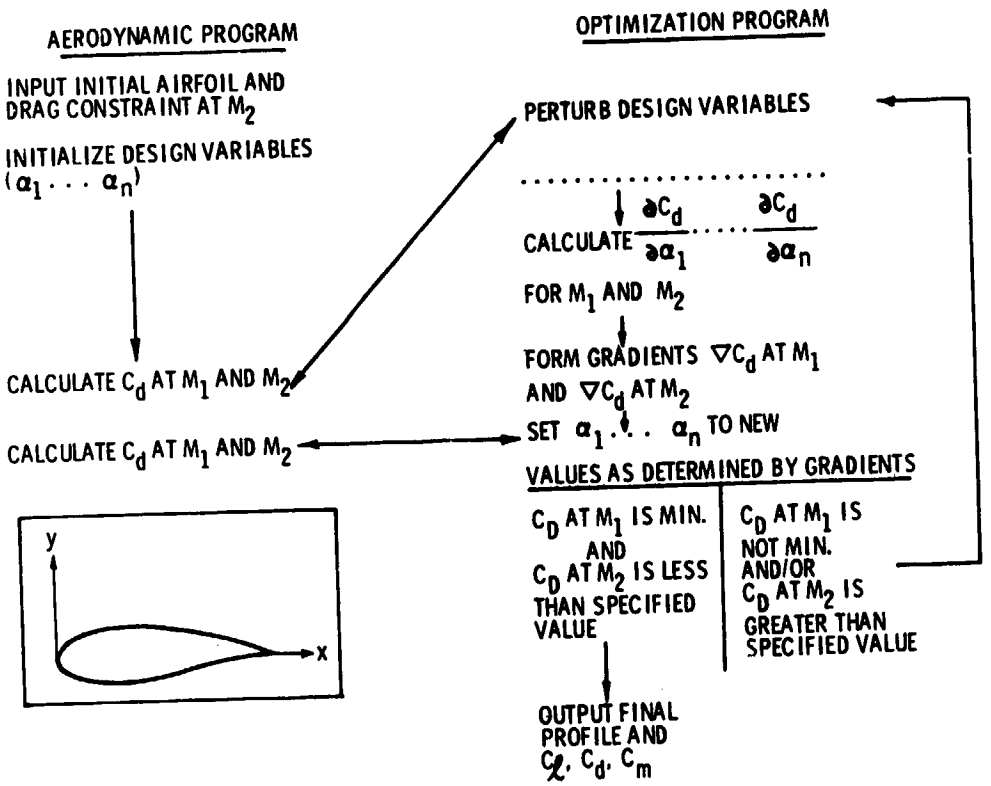

Figure 1.- Flow chart of numerical optimization design program.

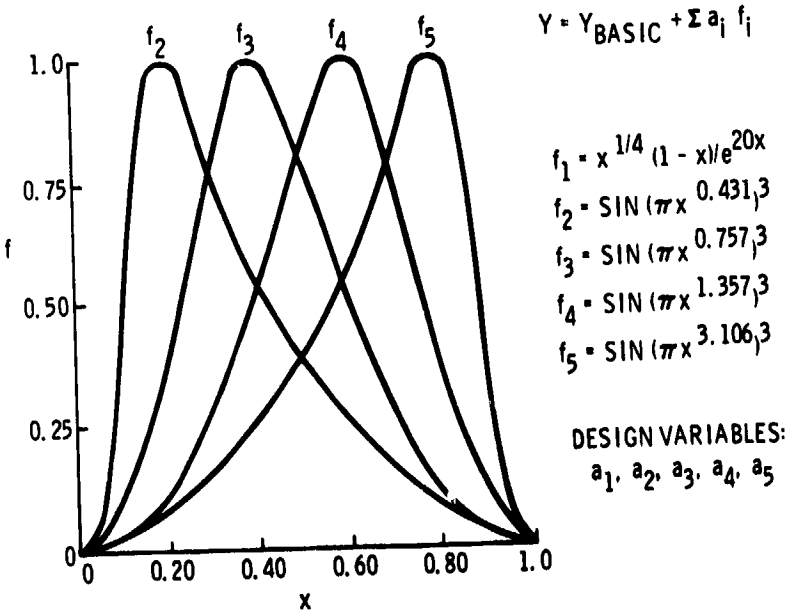

Figure 2.- Airfoil shape functions.

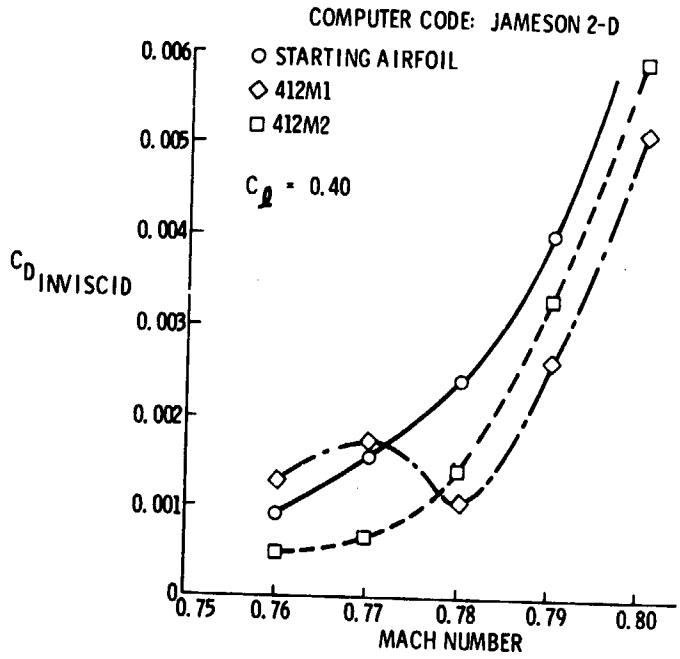

Figure 3.- Airfoil section optimization.

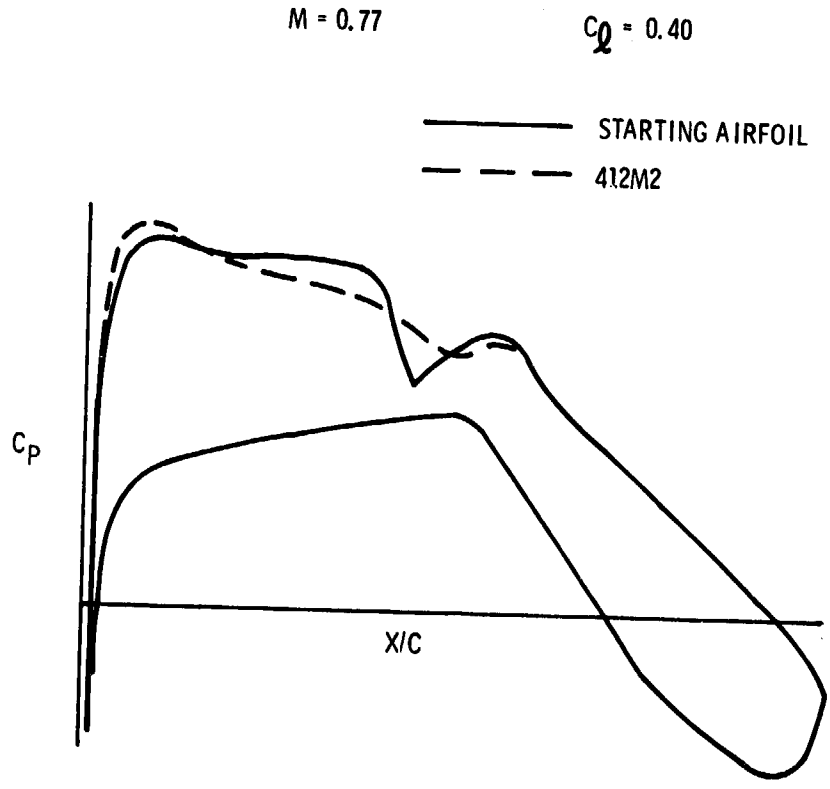

Figure 4.- Airfoil section pressure distributions.

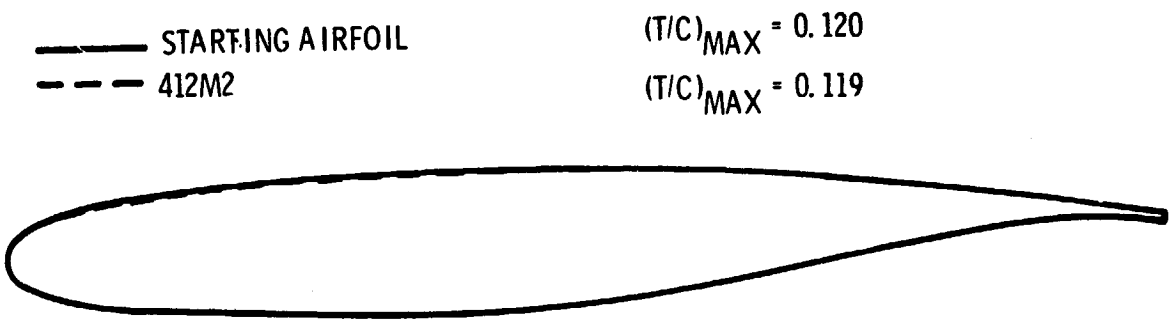

Figure 5.- Airfoil geometry comparison.

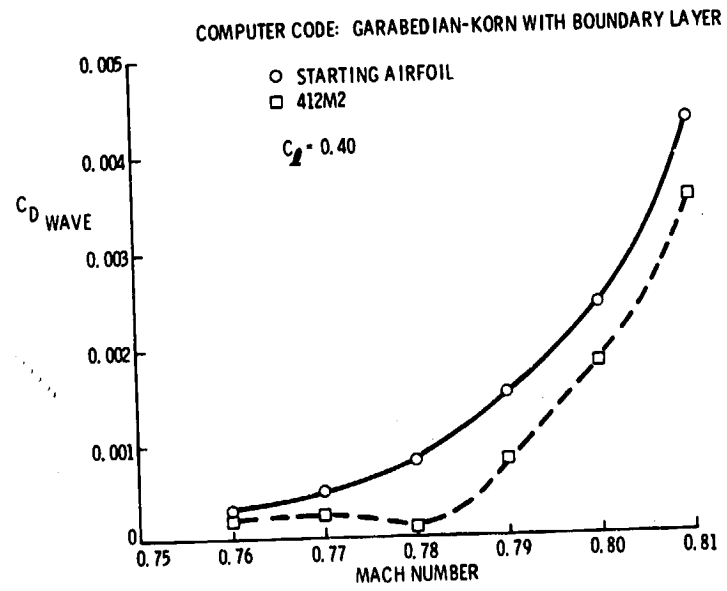

Figure 6.- Comparison of wave drag characteristics for the starting airfoil and optimized airfoil 412M2.

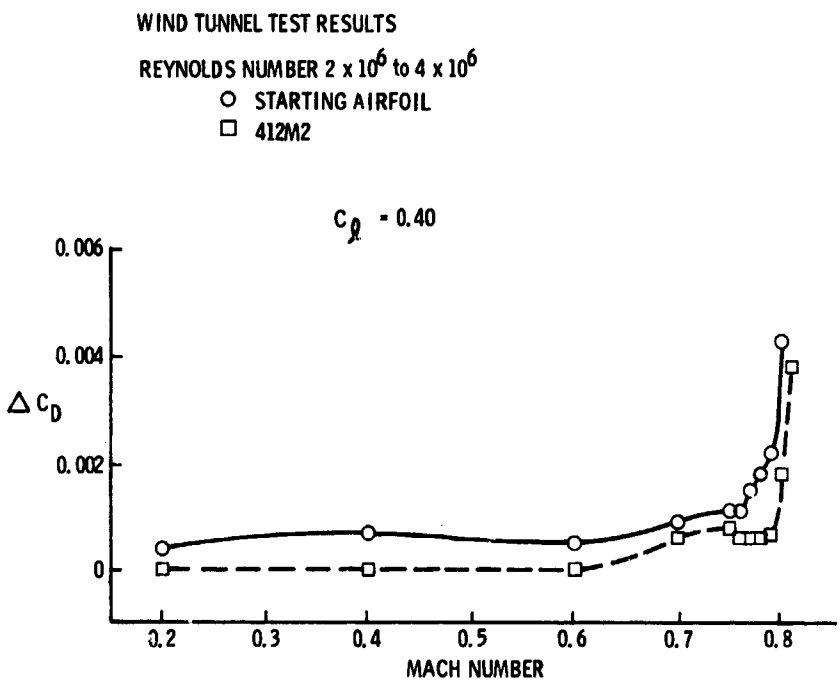

Figure 7.- Experimental drag characteristics for the starting airfoil and optimized airfoil 412M2 at C_ℓ = 0.40.

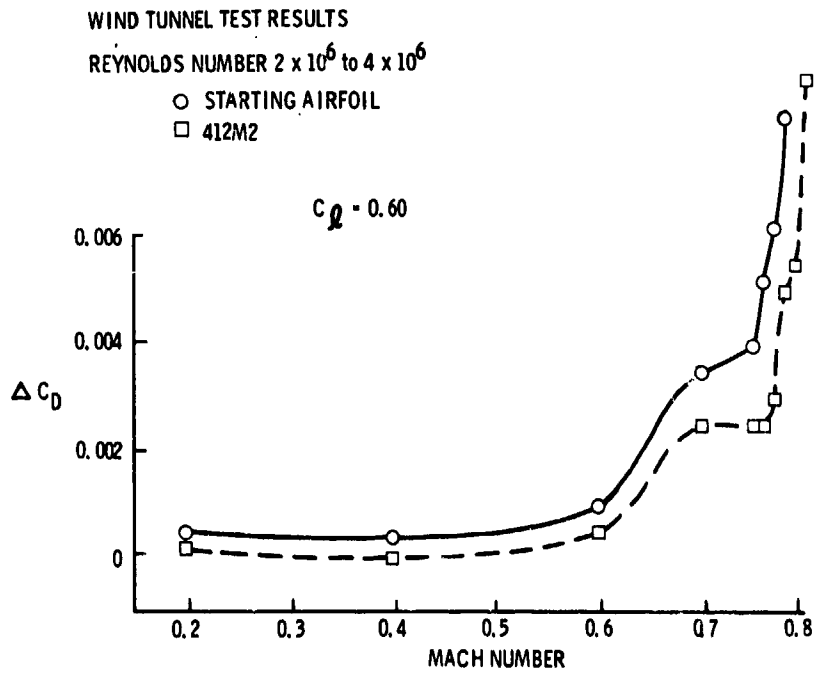

Figure 8.- Experimental drag characteristics for the starting airfoil and optimized airfoil 412M2 at C_ℓ = 0.60.